The nonlinear piezoelectric tuned vibration absorber

Soltani, P. S. & Kerschen, G.

Original citation & hyperlink:
Soltani, PS & Kerschen, G 2015, 'The nonlinear piezoelectric tuned vibration absorber' Smart Materials and Structures, vol. 24, no. 7, 075015
https://dx.doi.org/10.1088/0964-1726

DOI 10.1088/0964-1726
ISSN 0964-1726
ESSN 1361-665X

Publisher: IOP Publishing

The Nonlinear Piezoelectric Tuned Vibration Absorber

P. Soltani, G. Kerschen

Space Structures and Systems Laboratory
Department of Aerospace and Mechanical Engineering
University of Liège, Liège, Belgium
E-mail: payam.soltani, g.kerschen@ulg.ac.be

Abstract

This paper proposes a piezoelectric vibration absorber, termed the nonlinear piezoelectric tuned vibration absorber (NPTVA), for the mitigation of nonlinear resonances of mechanical systems. The new feature of the NPTVA is that its nonlinear restoring force is designed according to a principle of similarity, i.e., the NPTVA should be an electrical analog of the nonlinear host system. Analytical formulas for the NPTVA parameters are derived using the homotopy perturbation method. Doing so, a nonlinear generalization of Den Hartog's equal-peak tuning rule is developed for piezoelectric vibration absorbers.

Keywords: *vibration mitigation, nonlinear resonances, piezoelectric vibration absorber, principle of similarity, equal-peak method, homotopy perturbation.*

Corresponding author:
Payam Soltani
Space Structures and Systems Laboratory
Department of Aerospace and Mechanical Engineering
University of Liège
1 Chemin des Chevreuils (B52/3), B-4000 Liège, Belgium.
Email: payam.soltani@ulg.ac.be.

1 Introduction

Piezoelectric tuned vibration absorbers (PTVAs) represent interesting alternatives to mechanical tuned vibration absorbers in that they have no moving parts and they can be fine-tuned online to compensate any modeling errors [1]. PTVAs are implemented with a piezoelectric transducer (PZT) bonded to, or embedded in the structure and shunted with an electrical impedance. Resonant circuit shunting is considered where the inherent capacitance of the PZT is shunted with a resistor R and an inductor L. Different tuning rules for RL shunts were proposed in the literature. In [2], Hagood and von Flotow developed two strategies based on Den Hartog's fixed point method and on pole placement. Hogsberg and Krenk proposed a tuning rule that is a balanced compromise between these two design criteria [3]. Through the development of an equivalent mechanical model of a piezoelectric element, Yamada et al. [4] introduced a new approximate analytical expression for the damping parameter that improves the PTVA performance compared to the formulas in [2]. Closed-form expressions related to shunt performance were also derived in [5]. Because all the aforementioned tuning rules are approximate, an exact closed-form solution for the design of PTVAs was established in reference [6].

One inherent limitation of RL shunt circuits is that they are tuned to a specific resonance frequency. As a result, their performance may degrade if the resonant frequency is modified due to, e.g., design uncertainty, environmental conditions, ageing and nonlinearity. To enlarge the suppression bandwidth, a first attempt to use a nonlinear piezoelectric absorber was made in [7], but the authors observed no significant performance increase. Nonlinear semi-passive approaches based on the concept of switch shunting were then introduced. Two strategies, namely state switching [8] and synchronized switch damping [9], were proposed and further developed and improved [10–12]. Another type of nonlinear piezoelectric absorber characterized by an essential nonlinearity was introduced in [13] as the electrical realization of the nonlinear energy sink (NES). It was subsequently applied to mistuned bladed disks in [14]. The absence of a linear component in the nonlinear restoring force of the electrical NES precludes the existence of a preferential resonance frequency. This absorber can therefore extract energy from virtually any vibration mode of a structure [15]. Multimodal damping of mechanical structures can also be realized by distributing an array of piezoelectric elements interconnected through a passive circuit. A very interesting finding of the work of Dell'Isola and co-workers is that, if the shunt circuit is governed by equations analogous to those of the host structure [16], hence obeying a 'principle of similarity' according to the terminology used in [17], effective mitigation of all the mechanical modes of the host structure can be achieved. Electrical circuits analog to beam and plate structures were derived in [18] and [19], respectively.

With continual interest in expanding the performance envelope of engineering systems, nonlinear components are increasingly utilized in real-world applications. Mitigating the resonant vibrations of nonlinear structures is therefore becoming a problem of great practical significance. In this context, the objective of this study is to introduce a new piezoelectric vibration absorber, termed the nonlinear piezoelectric tuned vibration absorber (NPTVA). Unlike the previously-proposed nonlinear piezoelectric vibration absorbers, the nonlinear restoring force of the NPTVA is *tuned* according to the nonlinear restoring force

of the host structure. Specifically, we extend the principle of similarity to nonlinear systems and demonstrate that the NPTVA should be an electrical analog of the nonlinear host system for effective vibration mitigation.

This paper is organized as follows. Section 2 briefly reviews the exact closed-form solution for linear PTVAs and shows how nonlinearity in the host system can deteriorate their performance. Section 3 proposes a principle of similarity for nonlinear piezoelectric vibration absorbers. Analytical formulas for the nonlinear coefficient of the NPTVA are derived in Section 4 using the homotopy perturbation method. Section 5 discusses the NPTVA performance, and the conclusions of the present study are drawn in Section 6.

2 The linear piezoelectric tuned vibration absorber (LPTVA)

The NPTVA considered in the present study comprises a piezoelectric transducer and a series RL shunt circuit with a nonlinear capacitor. Because the RL parameters of the NPTVA will be tuned as in the linear case, this section briefly reviews the exact solution proposed for LPTVAs in [6].

2.1 LPTVA coupled to a linear oscillator: an exact tuning rule

A LPTVA is coupled to an undamped one-degree-of-freedom modal model of the host structure that represents the resonance of interest. The coupled system is depicted in Figure 1 and is subjected to harmonic forcing. The PZT transducer is considered as a one-dimensional PZT rod in which both the expansion and polarization directions coincide with the central axis of the rod (conventionally called '3-direction'). The capacitance of the PZT rod with no external forces c_{PZT} and its stiffness with short-circuited electrodes k_{PZT} are defined as:

$$c_{PZT} = \epsilon_3^T \frac{s_0}{l_0}, \quad k_{PZT} = \frac{1}{s_{33}^E} \frac{s_0}{l_0}, \tag{1}$$

where s_0 and l_0 are the cross section area and length of the PZT rod, respectively. ϵ_3^T and s_{33}^E are the permittivity under constant strain and the compliance under constant electric field of the PZT rod in 3-direction, respectively [20].

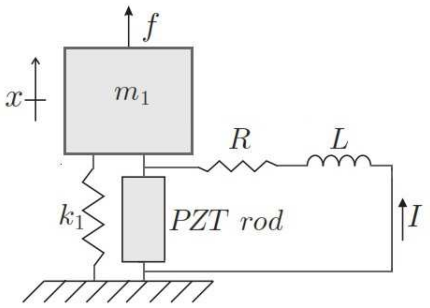

Figure 1: Piezoelectric vibration absorber with a series RL shunt.

The governing equations of the coupled system are written as:

$$\begin{aligned} m_1\ddot{x} + \left(k_1 + \overline{k}_{PZT}\right) x - \theta q &= f \sin \omega t, \\ L\ddot{q} + R\dot{q} + \overline{c}_{PZT}^{-1}\, q - \theta x &= 0, \end{aligned} \tag{2}$$

where

$$\overline{c}_{PZT} = c_{PZT}(1 - k_0^2), \quad \overline{k}_{PZT} = \frac{k_{PZT}}{1 - k_0^2}, \quad \theta = \frac{k_0}{1 - k_0^2}\sqrt{\frac{k_{PZT}}{c_{PZT}}}, \tag{3}$$

are the capacitance of the PZT rod under constant strain, the stiffness of the PZT rod with open electrodes, and the electromechanical coupling factor θ, respectively. k_0 is defined as the electromechanical coupling coefficient in d_{33}-mode:

$$k_0 = d_{33}\sqrt{\frac{k_{PZT}}{c_{PZT}}} = d_{33}\frac{1}{\sqrt{s_{33}^E \epsilon_3^T}}. \tag{4}$$

The governing equations (2) are recast into:

$$\begin{aligned} \widetilde{x}^{\,\prime\prime} + \widetilde{x} - \delta\alpha\widetilde{q} &= f_0 \sin \gamma\tau \\ \widetilde{q}^{\,\prime\prime} + r\delta^2\widetilde{q}^{\,\prime} - \delta\alpha\widetilde{x} + \delta^2\widetilde{q} &= 0, \end{aligned} \tag{5}$$

where prime denotes differentiation respect to the dimensionless time $\tau = \omega_1 t$ and the other parameters are defined as in [6] :

$$\begin{aligned} &\omega_1 = \sqrt{\frac{k_1 + \overline{k}_{PZT}}{m_1}}, \quad \omega_e = \frac{1}{\sqrt{L\ \overline{c}_{PZT}}}, && \gamma = \frac{\omega}{\omega_1}, && \delta = \frac{\omega_e}{\omega_1}, \\ &\widetilde{x} = \sqrt{m_1}\ x, && \widetilde{q} = \sqrt{L}\ q, && r = R\,\overline{c}_{PZT}\,\omega_1, \\ &\kappa = k_1/\overline{k}_{PZT}, && f_0 = \frac{f}{\omega_1\sqrt{\overline{k}_{PZT} + k_1}}, && \alpha = \theta\sqrt{\frac{\overline{c}_{PZT}}{\overline{k}_{PZT} + k_1}} = \frac{k_0}{\sqrt{1+\kappa}}. \end{aligned} \tag{6}$$

In practical applications, the dimensionless electromechanical coupling parameter α can take values between 0.1 and 0.3 (see, e.g., [21]), while its theoretical values could be up to 0.7 [6]. Given a value of this parameter, the tuning of the shunt requires to determine the frequency δ and damping r ratios in Equation (5). Reference [6] derived the values of δ and r which impose exactly two equal peaks in the receptance function that are associated with the smallest possible vibration amplitude of the host structure (H_∞ optimization):

$$\delta_{opt} = 2\sqrt{\frac{\tilde{a}}{4\,S\tilde{a} - \tilde{b}}}, \quad r_{opt} = \sqrt{\frac{2\left[1 + \left({\delta_{opt}}^2 + 1\right)\left(\alpha^2 + \chi - 1\right){h_0}^2\right]}{\left[1 + \left(\chi\,{\delta_{opt}}^2 - 1\right){h_0}^2\right]{\delta_{opt}}^2}}. \tag{7}$$

The resistance R and inductance L of the shunt circuit are calculated directly from r_{opt} and δ_{opt}:

$$\begin{aligned} L &= \frac{1}{\delta_{opt}^2}\frac{m_1}{(1+\kappa)\ \epsilon_3^T}\left(\frac{s_{33}\,l_0}{s_0}\right)^2, \\ R &= \frac{r_{opt}}{\epsilon_3^T}\sqrt{\frac{m_1}{1+\kappa}}\sqrt{s_{33}\left(\frac{l_0}{s_0}\right)^3}. \end{aligned} \tag{8}$$

An analytical expression for the amplitude of the resonance peaks h_0 was also obtained in [6]. It was found to depend only on the parameter α:

$$h_0 = \frac{8}{\alpha\sqrt{2\sqrt{54\,\alpha^4 - 144\,\alpha^2 + 64} + 9\,\alpha^2 + 16}}, \tag{9}$$

The auxiliary parameters in Equations (7) are given in Appendix A. The analytical expressions of the resonant frequencies γ_M and γ_N, which will be required in Section 4, are also derived in this Appendix.

2.2 LPTVA coupled to a nonlinear oscillator

To illustrate the detuning of the LPTVA in the presence of nonlinearity, a cubic nonlinearity is introduced in the equation governing the host oscillator:

$$\begin{aligned} \widetilde{x}'' + \widetilde{x} - \delta\alpha\widetilde{q} + k_3\tilde{x}^3 &= f_0 \sin\gamma\tau \\ \widetilde{q}'' + r\delta^2\widetilde{q}' - \delta\alpha\widetilde{x} + \delta^2\widetilde{q} &= 0, \end{aligned} \tag{10}$$

The frequency response of the coupled system is calculated using a path-following algorithm combining shooting and pseudo-arclength continuation [22]. Figure 2 represents the response of the host structure for different forcing amplitudes f_0. The nonlinear coefficient k_3 is equal to $k_3 = 10^{-5}$, and α is chosen to be equal to 0.2. The linear parameters $\delta = 1.00017$ and $r = 0.2491$ are computed according to Equations (7).

For $f_0 = 2$ in Figure 2(a), the system behaves linearly, and two peaks of equal amplitude are obtained in accordance with linear theory. When the forcing amplitude is increased, the cubic nonlinearity of the host system is activated and is responsible for a substantial increase in the resonance frequency of the second peak. For $f_0 = 8$ and beyond, unequal peaks are observed. As a result, the LPTVA is no longer effective due to the noticeable difference between the amplitudes of the resonances. For forcing amplitudes greater than $f_0 = 11.9$, e.g., for $f_0 = 12.5$ in Figure 2(b), a detached resonance curve connects to the main branch through the second resonance peak, which suddenly and drastically increases the amplitude of this peak. The complete peak is not shown in Figure 2(b), because its amplitude goes well beyond 100. Such a nonlinear dynamical phenomenon is therefore dangerous and must be avoided.

3 Principle of similarity for the NPTVA

A NPTVA is now considered for mitigating the vibrations of the cubic oscillator. An unconventional feature of the NPTVA is that the mathematical form of its nonlinear restoring force is not imposed a priori, as it is the case for most existing nonlinear absorbers. The equations of motion are therefore:

$$\begin{aligned} \widetilde{x}'' + \widetilde{x} - \delta\alpha\widetilde{q} + k_3\tilde{x}^3 &= f_0 \sin\gamma\tau, \\ \widetilde{q}'' + r\delta^2\widetilde{q}' - \delta\alpha\widetilde{x} + \delta^2\widetilde{q} + g(\widetilde{q}) &= 0, \end{aligned} \tag{11}$$

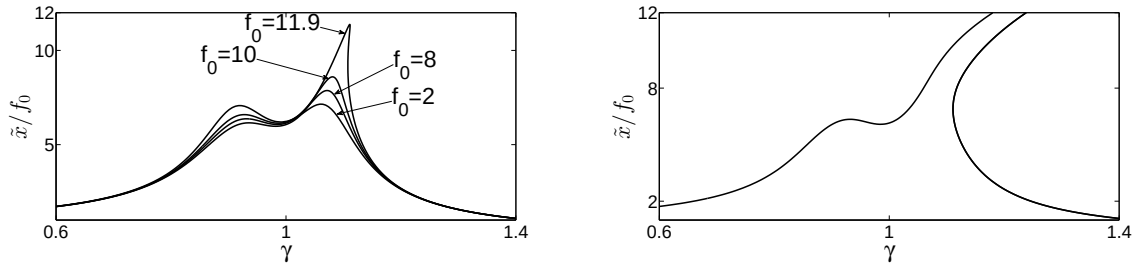

Figure 2: Frequency response of a nonlinear cubic oscillator with an attached LPTVA for different forcing amplitudes f_0 ($\alpha = 0.2$ and $k_3 = 10^{-5}$). (a) $f_0 < 12$; (b) $f_0 = 12.5$.

where $g(\widetilde{q})$ represents a nonlinear capacitor and is to be determined.

Reference [23], which examined the case of a nonlinear mechanical absorber coupled to a nonlinear mechanical structure, demonstrated that the absorber should be a 'mirror' of the host system for effective mitigation in a large range of forcing amplitudes. For instance, if the nonlinearity in the host system is quadratic or cubic, the absorber should possess a quadratic or a cubic spring, respectively. This mirror rule suggests that the NPTVA should be chosen such that the shunt is governed by an equation analogous to that of the host structure, thereby extending the principle of similarity described in [16–19] to nonlinear systems. Following this result, the coupled host and NPTVA system should be written:

$$\begin{aligned} \widetilde{x}'' + \widetilde{x} - \delta\alpha\widetilde{q} + k_3\tilde{x}^3 &= f_0 \sin\gamma\tau, \\ \widetilde{q}'' + r\delta^2\widetilde{q}' - \delta\alpha\widetilde{x} + \delta^2\widetilde{q} + \beta_3\tilde{q}^3 &= 0. \end{aligned} \tag{12}$$

One possible strategy to determine the nonlinear coefficient β_3 (or equivalently the nonlinear tuning parameter $m_3 = \beta_3/k_3$) is to find the value that realizes two equal peaks, for instance at $f_0 = 8$ when the LPTVA starts to be detuned. By trial and error, a value of $m_3 = 2.06$ was obtained for $k_3 = 10^{-5}$. Figure 3(a) illustrates the corresponding response of the host structure scaled by the forcing amplitude f_0. The result in this figure is remarkable for two reasons. First, not only equal peaks are obtained at $f_0 = 8$, but they are also observed at higher forcing amplitudes. This means that equal peaks can be maintained in a relatively large range of forcing amplitudes when a properly-tuned NPTVA is attached to a nonlinear oscillator. Second, the amplitudes of the resonance peaks in Figure 3(a) are barely affected by the forcing amplitude f_0, as if the coupled nonlinear system would obey the superposition principle.

A nonlinear oscillator with quintic spring and a quintic NPTVA was also studied:

$$\begin{aligned} \widetilde{x}'' + \widetilde{x} - \delta\alpha\widetilde{q} + k_5\tilde{x}^5 &= f_0 \sin\gamma\tau \\ \widetilde{q}'' + r\delta^2\widetilde{q}' - \delta\alpha\widetilde{x} + \delta^2\widetilde{q} + \beta_5\tilde{q}^5 &= 0, \end{aligned} \tag{13}$$

In this case, $m_5 = \beta_5/k_5$ should be equal to 4.11 to have equal peaks for $k_5 = 10^{-8}$ and $f_0 = 5$. Figure 3(b) confirms that qualitatively similar results are obtained for quintic nonlinearities, which further validates the theoretical findings of this section.

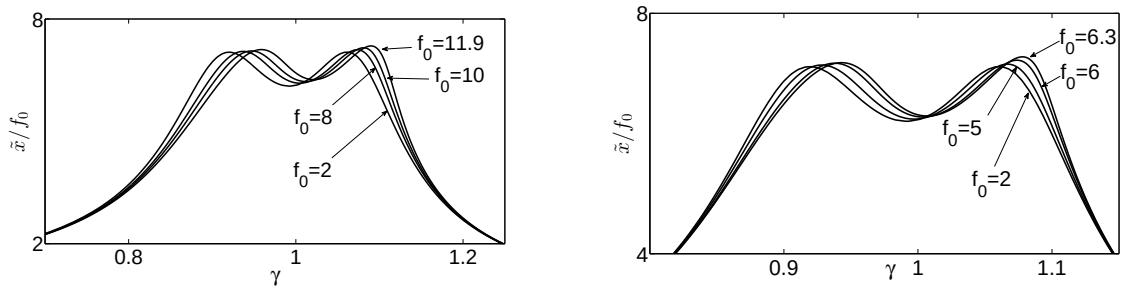

(a) (b)

Figure 3: Frequency response of a nonlinear oscillator with an attached NPTVA for different forcing amplitudes f_0. (a) Cubic NPTVA coupled to a cubic oscillator ($\alpha = 0.2$, $k_3 = 10^{-5}$ and $m_3 = 2.06$); (b) quintic NPTVA coupled to a quintic oscillator ($\alpha = 0.2$, $k_5 = 10^{-8}$ and $m_5 = 4.11$).

4 Analytical solution for the nonlinear equal-peak method

4.1 Homotopy perturbation method

Because the values of m_3 and m_5 were sought by trial and error in the previous section, the goal now is to establish accurate analytical approximations for these values. For generality, a host system with both cubic and quintic nonlinearities is considered. According to the principle of similarity, the NPTVA should also possess these two nonlinearities:

$$\begin{aligned} \widetilde{x}'' + \widetilde{x} - \delta\alpha\widetilde{q} + k_3\tilde{x}^3 + k_5\tilde{x}^5 &= f_0 \sin\gamma\tau, \\ \widetilde{q}'' + r\delta^2\widetilde{q}' - \delta\alpha\widetilde{x} + \delta^2\widetilde{q} + \beta_3\tilde{q}^3 + \beta_5\tilde{q}^5 &= 0. \end{aligned} \tag{14}$$

A one-term harmonic balance approximation, $\widetilde{x}(\tau) = A_1 \sin\gamma\tau + A_2 \cos\gamma\tau$ and $\widetilde{q}(\tau) = q_1 \sin\gamma\tau + q_2 \cos\gamma\tau$, is introduced into Equations (14). Applying the approximations

$$\begin{aligned} \cos^3(\gamma\,\tau) \simeq 3/4\cos(\gamma\,\tau), \quad \sin^3(\gamma\,\tau) \simeq 3/4\sin(\gamma\,\tau), \\ \cos^5(\gamma\,\tau) \simeq 5/8\cos(\gamma\,\tau), \quad \sin^5(\gamma\,\tau) \simeq 5/8\sin(\gamma\,\tau). \end{aligned} \tag{15}$$

and balancing sine and cosine coefficients yields the nonlinear algebraic equation:

$$\mathbf{G}(\mathbf{X}) \equiv \mathbf{M}\,\mathbf{X} + \mathbf{NL}(\mathbf{X}) - \mathbf{F} = \mathbf{0}, \tag{16}$$

where $\mathbf{X}$ and $\mathbf{F}$ are the displacement and force vectors, respectively, and $\mathbf{M}$ contains the linear parameters of the coupled system:

$$\mathbf{X} = \begin{Bmatrix} A_1 \\ A_2 \\ q_1 \\ q_2 \end{Bmatrix}, \mathbf{F} = \begin{Bmatrix} 0 \\ f_0 \\ 0 \\ 0 \end{Bmatrix}, \mathbf{M} = \begin{bmatrix} 0 & -\gamma^2+1 & 0 & -\alpha\,\delta \\ -\gamma^2+1 & 0 & -\alpha\,\delta & 0 \\ 0 & -\alpha\,\delta & -\delta^2\gamma\,r & \delta^2-\gamma^2 \\ -\alpha\,\delta & 0 & \delta^2-\gamma^2 & \delta^2\gamma\,r \end{bmatrix}. \tag{17}$$

The nonlinear terms are gathered in $\mathbf{NL}$:

$$\mathbf{NL} = \left\{ \begin{array}{c} \left[\frac{1}{8}\left(5\,{A_1}^4 - 10\,{A_1}^2{A_2}^2 + {A_2}^4\right)A_2 + \frac{1}{4}\left(10\,{A_1}^2{A_2}^2 - 2\,{A_2}^4\right)A_2 + {A_2}^5\right]k_5 + \\ \left[\frac{1}{4}\left(3\,{A_1}^2 - {A_2}^2\right)A_2 + {A_2}^3\right]k_3 \\ \left[\frac{5}{8}A_1\,\left({A_1}^4 - 10\,{A_1}^2{A_2}^2 + 5\,{A_2}^4\right) + \frac{15}{2}\,{A_1}^3{A_2}^2 - \frac{5}{2}\,A_1\,{A_2}^4\right]k_5 + \\ \left[\frac{3}{4}\,{A_1}^3 + \frac{3}{4}\,A_1\,{A_2}^2\right]k_3 \\ \left[\frac{1}{8}\,\left(5\,{q_1}^4 - 10\,{q_1}^2{q_2}^2 + {q_2}^4\right)q_2 + \frac{1}{4}\,\left(10\,{q_1}^2{q_2}^2 - 2\,{q_2}^4\right)q_2 + {q_2}^5\right]\beta_5 + \\ \left[\frac{1}{4}\,\left(3\,{q_1}^2 - {q_2}^2\right)q_2 + {q_2}^3\right]\beta_3 \\ \left[\frac{5}{8}\,q_1\,\left({q_1}^4 - 10\,{q_1}^2{q_2}^2 + 5\,{q_2}^4\right) + \frac{15}{2}\,{q_1}^3{q_2}^2 - \frac{5}{2}\,q_1\,{q_2}^4\right]\beta_5 + \\ \left[\frac{3}{4}\,{q_1}^3 + \frac{3}{4}\,q_1\,{q_2}^2\right]\beta_3 \end{array} \right\}. \tag{18}$$

We propose to solve Equation (16) using the homotopy perturbation method (HPM) [24, 25]. Compared to traditional perturbation methods [26], HPM does not require the definition of a small perturbation parameter and was found in the literature to be accurate enough at strong nonlinear regimes. The method starts by constructing a homotopy function for $\mathbf{G}(\mathbf{X})$:

$$\mathbf{H}(\mathbf{X}; p) = (1-p)[\mathbf{M}\,\mathbf{X} - \mathbf{F} - \mathbf{M}\,\mathbf{X}_0] + p\,\mathbf{G}(\mathbf{X}), \tag{19}$$

where $\mathbf{X}_0$ is an initial guess, and $p \in [0, 1]$ is the homotopy parameter. By enforcing $\mathbf{H}(\mathbf{X}; p) = \mathbf{0}$ and by varying p from 0 to 1, a family of algebraic equations is created, the solution of which evolves continuously from the initial linear system to the solution of the considered nonlinear system.

Expanding the solution $\mathbf{X}$ around $p = 0$, the approximate solution $\widehat{\mathbf{X}}(p)$ is expressed as a so-called homotopy series:

$$\widehat{\mathbf{X}}(p) = \mathbf{X}_0 + \sum_{i=1}^{\infty} p^i\,\widehat{\mathbf{X}}_i, \tag{20}$$

Assuming that this series converges at $p = 1$ [27], i.e., $\widehat{\mathbf{X}}(1) = \mathbf{X}$, the analytical solution is described as:

$$\mathbf{X} = \mathbf{X}_0 + \sum_{i=1}^{\infty} \widehat{\mathbf{X}}_i. \tag{21}$$

Substituting the approximation (20) into $\mathbf{H}(\widehat{\mathbf{X}}; p) = 0$, considering $\mathbf{X}_0 = 0$ and equating terms of the same power of p yields:

$$(p^i) : \widehat{\mathbf{X}}_i = \left\{ \begin{array}{c} A_{1i} \\ A_{2i} \\ q_{1i} \\ q_{2i} \end{array} \right\} = \mathbf{M}^{-1} \times \mathbf{C}_i. \quad i = 1, 2, ... \tag{22}$$

The first six terms of the series are:

$$\mathbf{C}_1 = \left\{ \begin{array}{c} 0 \\ f_0 \\ 0 \\ 0 \end{array} \right\}, \; \mathbf{C}_2 = \mathbf{C}_3 = \mathbf{C}_5 = 0,$$

$$\mathbf{C}_4 = \left\{ \begin{array}{c} -\frac{3}{4}\, A_{21} \left({A_{11}}^2 + {A_{21}}^2 \right) k_3 \\ -\frac{3}{4}\, A_{11} \left({A_{11}}^2 + {A_{21}}^2 \right) k_3 \\ -\frac{3}{4}\, q_{21} \left({q_{11}}^2 + {q_{21}}^2 \right) \beta_3 \\ -\frac{3}{4}\, q_{11} \left({q_{11}}^2 + {q_{21}}^2 \right) \beta_3 \end{array} \right\}, \; \mathbf{C}_6 = \left\{ \begin{array}{c} -\frac{5}{8}\, A_{21} \left({A_{11}}^2 + {A_{21}}^2 \right)^2 k_5 \\ -\frac{5}{8}\, A_{11} \left({A_{11}}^2 + {A_{21}}^2 \right)^2 k_5 \\ -\frac{5}{8}\, q_{21} \left({q_{11}}^2 + {q_{21}}^2 \right)^2 \beta_5 \\ -\frac{5}{8}\, q_{11} \left({q_{11}}^2 + {q_{21}}^2 \right)^2 \beta_5 \end{array} \right\}. \quad (23)$$

Equations (21-23) therefore provide an approximate solution to Equation (16):

$$\mathbf{X} = \left\{ \begin{array}{c} A_1 \\ A_2 \\ q_1 \\ q_2 \end{array} \right\} = \mathbf{M}^{-1} \times \sum_{i=1}^{6} \mathbf{C}_i. \quad (24)$$

We note that in the absence of quintic terms ($k_5 = \beta_5 = 0$), the nonzero terms are limited to $\widehat{\mathbf{X}}_1$ and $\widehat{\mathbf{X}}_4$. In the absence of cubic terms ($k_3 = \beta_3 = 0$), the nonzero terms are $\widehat{\mathbf{X}}_1$ and $\widehat{\mathbf{X}}_6$. It can be shown that coupling between cubic and quintic nonlinearities do not appear before the term $\widehat{\mathbf{X}}_9$.

4.2 Proposed analytical tuning rule for the NPTVA

Based on the analytical developments in the previous section, we propose to extend Den Hartog's equal-peak method to nonlinear systems using the NPVTA. The amplitudes of the response of the host structure at the two linear resonant frequencies γ_M and γ_N should therefore be equated:

$$\sqrt{A_1^2(\gamma_M) + A_2^2(\gamma_M)} = \sqrt{A_1^2(\gamma_N) + A_2^2(\gamma_N)}, \quad (25)$$

which is rewritten as

$$F \equiv (A_{1N}^2 - A_{1M}^2) + (A_{2N}^2 - A_{2M}^2) = 0, \quad (26)$$

where subscripts M and N indicate that the corresponding quantity should be calculated at the resonant frequency γ_M or γ_N, respectively.

For simplicity, the resonant frequencies γ_M and γ_N of the underlying linear system, given in Appendix A, are used to locate the resonance peaks of the nonlinear system. Since nonlinearities shift the location of resonances, this represents an approximation. Ideally, the resonance frequencies of the nonlinear system should be two additional unknowns, and conditions expressing that the transfer function is maximum at these frequencies should be considered. Nonetheless, as we shall see later, this approximation does not significantly affect the predictive capabilities of the proposed analytical developments.

4.2.1 Cubic nonlinearities

The case where the coupled system presents only cubic nonlinearities is first analyzed, and the approximation $\mathbf{M}^{-1} \times (\mathbf{C}_1 + \mathbf{C}_4)$ is considered. In this case, the coefficients A_1

and A_2 can be rewritten as:

$$\left\{ \begin{array}{c} A_1 \\ A_2 \end{array} \right\} = \left[\begin{array}{cc} a_1 & b_1 \\ a_2 & b_2 \end{array} \right] \left\{ \begin{array}{c} k_3 \\ \beta_3 \end{array} \right\} + \left\{ \begin{array}{c} c_1 \\ c_2 \end{array} \right\}. \tag{27}$$

where

$$\begin{aligned}
a_1 &= \frac{3}{4} \frac{\left({A_{11}}^2 + {A_{21}}^2\right)}{Y_0} \left\{ \begin{array}{c} \left\{ \begin{array}{c} [\gamma^4 r^2 + (-r^2+1)\,\gamma^2 + \alpha^2 - 1]\delta^4 + \\ [-2\,\gamma^4 + (-\alpha^2+2)\,\gamma^2]\,\delta^2 + \gamma^6 - \gamma^4 \end{array} \right\} A_{11} + \\ \gamma\, r A_{21}\, \alpha^2 \delta^4 \end{array} \right\}, \\
a_2 &= \frac{3}{4} \frac{\left({A_{11}}^2 + {A_{21}}^2\right)}{Y_0} \left\{ \begin{array}{c} \left\{ \begin{array}{c} [\gamma^4 r^2 + (-r^2+1)\,\gamma^2 + \alpha^2 - 1]\delta^4 + \\ [-2\,\gamma^4 + (-\alpha^2+2)\,\gamma^2]\,\delta^2 + \gamma^6 - \gamma^4 \end{array} \right\} A_{21} - \\ \gamma\, r A_{11}\, \alpha^2 \delta^4 \end{array} \right\}, \\
b_1 &= \frac{-3}{4} \frac{\left({q_{11}}^2 + {q_{21}}^2\right)}{Y_0} \left\{ \begin{array}{c} [(-\alpha^2 - \gamma^2 + 1)\,\delta^2 + \gamma^4 - \gamma^2] q_{11} + \\ \gamma\, r \delta^2\, (\gamma^2 - 1)\, q_{21} \end{array} \right\} \alpha\, \delta, \\
b_2 &= \frac{-3}{4} \frac{\left({q_{11}}^2 + {q_{21}}^2\right)}{Y_0} \left\{ \begin{array}{c} [(-\alpha^2 - \gamma^2 + 1)\,\delta^2 + \gamma^4 - \gamma^2] q_{21} - \\ \gamma\, r \delta^2\, (\gamma^2 - 1)\, q_{11} \end{array} \right\} \alpha\, \delta, \\
c_1 &= -\frac{f_0}{Y_0} \left\{ \left[\gamma^4 r^2 + \left(-r^2+1\right)\gamma^2 + \alpha^2 - 1\right] \delta^4 - \gamma^2 \left(\alpha^2 + 2\,\gamma^2 - 2\right) \delta^2 + \gamma^6 - \gamma^4 \right\}, \\
c_2 &= \frac{r \alpha^2 \delta^4 \gamma\, f_0}{Y_0},
\end{aligned} \tag{28}$$

with

$$\begin{aligned}
Y_0 &= [r^2 \gamma^6 + (-2\,r^2 + 1)\,\gamma^4 + (2\,\alpha^2 + r^2 - 2)\,\gamma^2 + \alpha^4 - 2\,\alpha^2 + 1]\,\delta^4 \\
&\quad -2\,\gamma^2\,(\gamma^2 - 1)\,(\alpha^2 + \gamma^2 - 1)\,\delta^2 + \gamma^8 - 2\,\gamma^6 + \gamma^4.
\end{aligned} \tag{29}$$

The advantage of Equation (27) is that it shows explicitly the dependence on the cubic and linear terms. Similarly, the function F in Equation (26) can be rewritten as:

$$F = F_L + F_{NL_3}, \tag{30}$$

with

$$F_L = c_{1N}^2 - c_{1M}^2 + c_{2N}^2 - c_{2M}^2, \tag{31}$$

and

$$\begin{aligned}
F_{NL_3} &= \left(b_{1M}^2 - b_{1N}^2 + b_{2M}^2 - b_{2N}^2\right) {\beta_3}^2 \\
&+ \left[\begin{array}{c} (2\,a_{1M}\,b_{1M} - 2\,a_{1N}\,b_{1N} + 2\,a_{2M}\,b_{2M} - 2\,a_{2N}\,b_{2N})\,k_3 + \\ 2\,c_{1M}\,b_{1M} - 2\,c_{1N}\,b_{1N} + 2\,c_{2M}\,b_{2M} - 2\,c_{2N}\,b_{2N} \end{array} \right] \beta_3 \\
&+ \left(a_{1M}^2 - a_{1N}^2 + a_{2M}^2 - a_{2N}^2\right) k_3^2 \\
&+ (2\,c_{1M}\,a_{1M} - 2\,c_{1N}\,a_{1N} + 2\,c_{2M}\,a_{2M} - 2\,c_{2N}\,a_{2N})\,k_3.
\end{aligned} \tag{32}$$

where again subscripts M and N indicate that the corresponding quantity should be calculated at the resonant frequency γ_M or γ_N, respectively.

If δ and r are chosen according to Equations (7), equal peaks are obtained in the linear case, which means that $F_L = 0$. Consequently, the equal-peak method can be extended

to nonlinear systems by enforcing $F_{NL_3} = 0$. Doing so, the expression of β_3 is obtained by solving the quadratic polynomial in (32), which yields:

$$\begin{aligned} m_{3\,opt} &= \frac{\beta_{3\,opt}}{k_3} = \frac{\sqrt{\Delta_3} - \left[\begin{array}{c} (2\,a_{1M}\,b_{1M} - 2\,a_{1N}\,b_{1N} + 2\,a_{2M}\,b_{2M} - 2\,a_{2N}\,b_{2N})\,k_3 + \\ 2\,c_{1M}\,b_{1M} - 2\,c_{1N}\,b_{1N} + 2\,c_{2M}\,b_{2M} - 2\,c_{2N}\,b_{2N} \end{array} \right]}{2\,k_3\left({b_{1M}}^2 - {b_{1N}}^2 + {b_{2M}}^2 - {b_{2N}}^2\right)}, \\ \Delta_3 &= \left[\begin{array}{c} (2\,a_{1M}\,b_{1M} - 2\,a_{1N}\,b_{1N} + 2\,a_{2M}\,b_{2M} - 2\,a_{2N}\,b_{2N})\,k_3 + \\ 2\,c_{1M}\,b_{1M} - 2\,c_{1N}\,b_{1N} + 2\,c_{2M}\,b_{2M} - 2\,c_{2N}\,b_{2N} \end{array} \right]^2 \\ &- 4({b_{1M}}^2 - {b_{1N}}^2 + {b_{2M}}^2 - {b_{2N}}^2) \\ &\times \left[\begin{array}{c} (a_{1M}^2 - a_{1N}^2 + a_{2M}^2 - a_{2N}^2)\,k_3^2 + \\ (2\,c_{1M}\,a_{1M} - 2\,c_{1N}\,a_{1N} + 2\,c_{2M}\,a_{2M} - 2\,c_{2N}\,a_{2N})\,k_3 \end{array} \right]. \end{aligned} \tag{33}$$

For validation, Table 1 compares the value of m_3 predicted by Equations (33) to the value obtained through direct numerical simulations in which equal peaks were enforced by trial and error. As it can be seen from this table, an excellent agreement is obtained between the two values. However, we note that the value predicted by the analytical formula decreases slightly for increasing f_0, whereas it is found to slightly increase in actuality. This discrepancy should be attributed to the different approximations performed in this section, namely the one-term harmonic balance expansion, the truncation of the homotopy series and the location of the nonlinear resonances using the linear resonant frequencies.

Table 1: Comparison between the analytical and numerical values of $m_{3\,opt}$ that realize equal peaks ($\alpha = 0.2$, $k_3 = 10^{-5}$).

f_0	$m_{3\,opt}$ - analytical	$m_{3\,opt}$ - numerical
4	2.05	2.02
6	2.03	2.03
8	2.01	2.06
10	1.99	2.08
12	1.96	2.12

4.2.2 Quintic nonlinearities

The case where the coupled system presents only quintic nonlinearities is now analyzed, and the approximation $\mathbf{M}^{-1} \times (\mathbf{C}_1 + \mathbf{C}_6)$ is considered. The coefficients A_1 and A_2 can be rewritten as:

$$\left\{ \begin{array}{c} A_1 \\ A_2 \end{array} \right\} = \left[\begin{array}{cc} d_1 & e_1 \\ d_2 & e_2 \end{array} \right] \left\{ \begin{array}{c} k_5 \\ \beta_5 \end{array} \right\} + \left\{ \begin{array}{c} c_1 \\ c_2 \end{array} \right\}, \tag{34}$$

where

$$
\begin{aligned}
d_1 &= \frac{5}{8}\frac{\left({A_{11}}^2+{A_{21}}^2\right)^2}{Y_0}\left\{\begin{array}{c}\left\{\begin{array}{c}[\gamma^4 r^2+(-r^2+1)\,\gamma^2+\alpha^2-1]\delta^4+\\ [-2\,\gamma^4+(-\alpha^2+2)\,\gamma^2]\,\delta^2+\gamma^6-\gamma^4\end{array}\right\}A_{11}+\\ \gamma\, r A_{21}\,\alpha^2\delta^4\end{array}\right\},\\
d_2 &= \frac{5}{8}\frac{\left({A_{11}}^2+{A_{21}}^2\right)^2}{Y_0}\left\{\begin{array}{c}\left\{\begin{array}{c}[\gamma^4 r^2+(-r^2+1)\,\gamma^2+\alpha^2-1]\delta^4+\\ [-2\,\gamma^4+(-\alpha^2+2)\,\gamma^2]\,\delta^2+\gamma^6-\gamma^4\end{array}\right\}A_{21}-\\ \gamma\, r A_{11}\,\alpha^2\delta^4\end{array}\right\},\\
e_1 &= \frac{-5}{8}\frac{\left({q_{11}}^2+{q_{21}}^2\right)^2}{Y_0}\left\{[\left(-\alpha^2-\gamma^2+1\right)\delta^2+\gamma^4-\gamma^2]q_{11}+\gamma\, r\delta^2 q_{21}\,\left(\gamma^2-1\right)\right\}\alpha\,\delta,\\
e_2 &= \frac{-5}{8}\frac{\left({q_{11}}^2+{q_{21}}^2\right)^2}{Y_0}\left\{[\left(-\alpha^2-\gamma^2+1\right)\delta^2+\gamma^4-\gamma^2]q_{21}+\gamma\, r\delta^2 q_{11}\,\left(\gamma^2-1\right)\right\}\alpha\,\delta.
\end{aligned}
\tag{35}
$$

The function F can be separated into

$$
F = F_L + F_{NL_5}, \tag{36}
$$

where

$$
\begin{aligned}
F_{NL_5} &= \left(e_{1M}^2-e_{1N}^2+e_{2M}^2-e_{2N}^2\right){\beta_5}^2\\
&+ \left[\begin{array}{c}(2\,d_{1M}\,e_{1M}-2\,d_{1N}\,e_{1N}+2\,d_{2M}\,e_{2M}-2\,d_{2N}\,e_{2N})\,k_5+\\ 2\,e_{1M}\,c_{1M}-2\,e_{1N}\,c_{1N}+2\,e_{2M}\,c_{2M}-2\,e_{2N}\,c_{2N}\end{array}\right]\beta_5\\
&+ \left(d_{1M}^2-d_{1N}^2+d_{2M}^2-d_{2N}^2\right)k_5^2\\
&+ (2\,c_{1M}\,d_{1M}-2\,c_{1N}\,d_{1N}+2\,c_{2M}\,d_{2M}-2\,c_{2N}\,d_{2N})\;k_5\\
&= 0
\end{aligned}
\tag{37}
$$

and, hence,

$$
\begin{aligned}
m_{5\,opt} &= \frac{\beta_{5\,opt}}{k_5} = \frac{\sqrt{\Delta_5}-\left[\begin{array}{c}(2\,d_{1M}\,e_{1M}-2\,d_{1N}\,e_{1N}+2\,d_{2M}\,e_{2M}-2\,d_{2N}\,e_{2N})\,k_5+\\ 2\,e_{1M}\,c_{1M}-2\,e_{1N}\,c_{1N}+2\,e_{2M}\,c_{2M}-2\,e_{2N}\,c_{2N}\end{array}\right]}{2\,k_5\,(e_{1M}^2-e_{1N}^2+e_{2M}^2-e_{2N}^2)},\\
\Delta_5 &= \left[\begin{array}{c}(2\,d_{1M}\,e_{1M}-2\,d_{1N}\,e_{1N}+2\,d_{2M}\,e_{2M}-2\,d_{2N}\,e_{2N})\,k_5+\\ 2\,e_{1M}\,c_{1M}-2\,e_{1N}\,c_{1N}+2\,e_{2M}\,c_{2M}-2\,e_{2N}\,c_{2N}\end{array}\right]^2\\
&- 4\left(e_{1M}^2-e_{1N}^2+e_{2M}^2-e_{2N}^2\right)\\
&\times \left[\begin{array}{c}\left(d_{1M}^2-d_{1N}^2+d_{2M}^2-d_{2N}^2\right)k_5^2\\ (2\,c_{1M}\,d_{1M}-2\,c_{1N}\,d_{1N}+2\,c_{2M}\,d_{2M}-2\,c_{2N}\,d_{2N})\;k_5\end{array}\right].
\end{aligned}
\tag{38}
$$

Table 2 shows that the analytical expression (38) for the quintic coefficient of the NPTVA is an excellent approximation to the exact value obtained through numerical simulations.

We note that more compact formulas for $m_{3\,opt}$ and $m_{5\,opt}$ are provided in Appendix B. These formulas provide rapid computation of these parameters, which could prove useful, for instance, for a digital implementation of the shunt circuit.

Table 2: Comparison between the analytical and numerical values of $m_{5\,opt}$ that realize equal peaks ($\alpha = 0.2$, $k_5 = 10^{-8}$).

f_0	$m_{5\,opt}$ - analytical	$m_{5\,opt}$ - numerical
3	4.13	4.10
4	4.12	4.10
5	4.10	4.11
6	4.06	4.19
7	4.04	4.4

5 NPTVA performance

For a given host system and a given electromechanical coupling parameter α, Equations (7) and (33) provide a generalization of Den Hartog's equal-peak method for cubic host structures. Likewise, Equations (7) and (38) generalize the equal-peak method for quintic host structures.

To demonstrate the performance of the NPTVA tuned using the analytical solution, Figure 4 displays the frequency response of the cubic oscillator computed using numerical simulations with the cubic coefficient of the NPTVA predicted by Equation (33). Regardless of the values of f_0, two peaks of almost equal amplitudes are obtained, which provides further evidence of the accuracy of the analytical formula. In this figure, we also note the performance improvement brought by the NPTVA compared to the LPTVA. Figure 5 plots the same result but for quintic nonlinearity.

Since the values of $m_{3\,opt}$ and $m_{5\,opt}$ vary with forcing amplitude in Figures 4 and 5, one may wonder whether a single value of the nonlinear coefficient in the NPTVA can also be effective for different forcing amplitudes. Figure 3, which was discussed in Section 3, confirms that it is indeed the case if, e.g., $m_3 = 2.06$ and $m_5 = 4.11$ for the cubic and quintic systems, respectively.

For a more quantitative comparison between the LPTVA and the NPTVA, the amplitudes of the resonant peaks of the host oscillator are compared in Figure 6 as a function of f_0. Figures 6(a,b) reveal that, unlike the LPTVA, the amplitudes of the two resonance peaks of the host system with an attached NPTVA remain almost identical. In addition, an interesting observation is that these amplitudes seem linearly related to the forcing amplitude, meaning that considering a properly-tuned nonlinearity in a shunt circuit connected to an already nonlinear system can give rise to linear-like behaviors and operational domain of the forcing amplitudes. Figures 6(c,d) illustrate that the NPTVA performance is always superior to that of the LPTVA, which is an appealing feature of this device.

Now we consider a host system possessing both cubic and quintic nonlinearities, i.e, $k_3\widetilde{x}^3 + k_5\widetilde{x}^5$ with $k_3 = 1 \times 10^{-5}$ and $k_5 = 1 \times 10^{-8}$, for, e.g., $f_0 = 4.1$. If we attach a cubic NPTVA as in Figure 7(a) or a quintic NPTVA as in Figure 7(b), two resonance peaks of unequal amplitudes are obtained. It is only when we attach a NPTVA with both

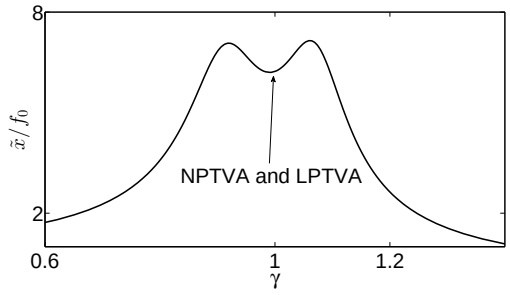

(a) $f_0 = 2, m_{3\,opt} = 2.05$

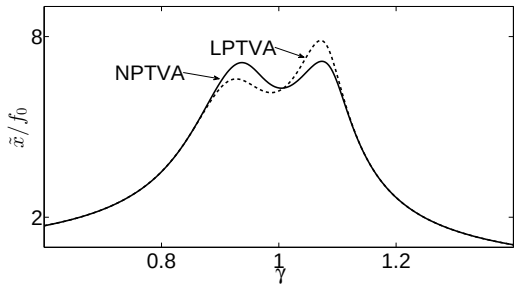

(b) $f_0 = 8, m_{3\,opt} = 2.01$

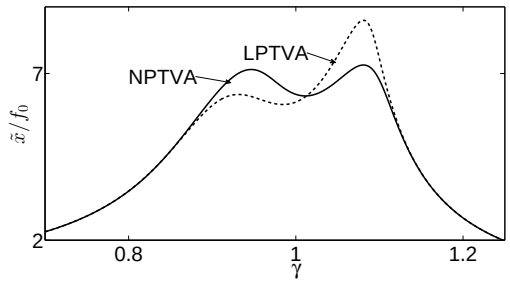

(c) $f_0 = 10, m_{3\,opt} = 1.99$

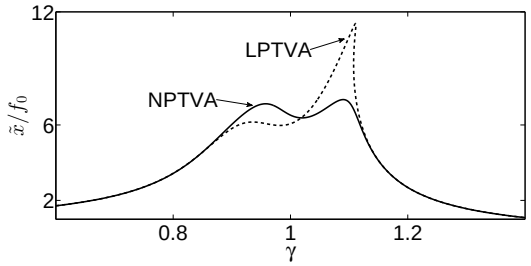

(d) $f_0 = 12, m_{3\,opt} = 1.96$

Figure 4: Frequency response of a cubic oscillator ($\alpha = 0.2$, $k_3 = 10^{-5}$) with a cubic NPTVA tuned using Equations (7) and (33).

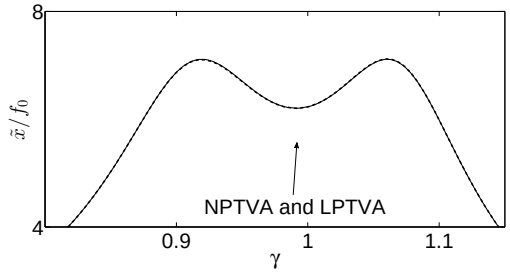

(a) $f_0 = 2, m_{5\,opt} = 4.14$

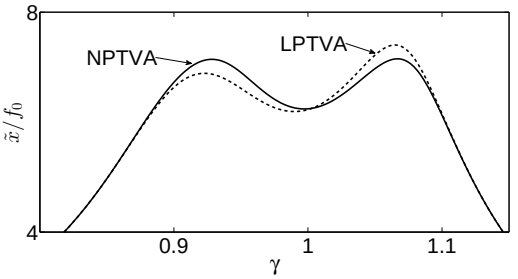

(b) $f_0 = 5, m_{5\,opt} = 4.10$

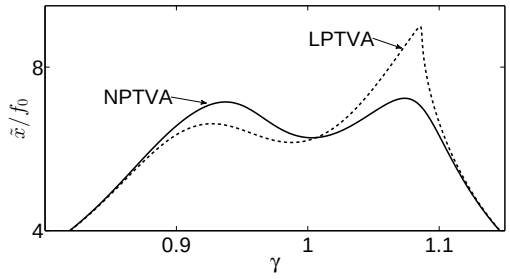

(c) $f_0 = 6, m_{5\,opt} = 4.06$

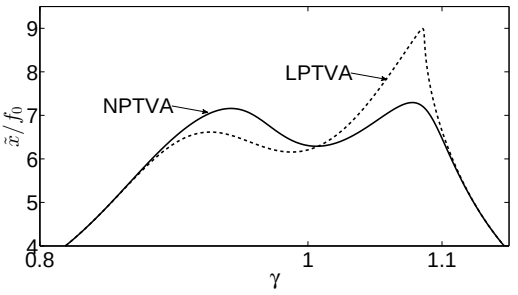

(d) $f_0 = 7, m_{5\,opt} = 4.04$

Figure 5: Frequency response of a quintic oscillator ($\alpha = 0.2$, $k_3 = 10^{-8}$) with a quintic NPTVA tuned using Equations (7) and (38).

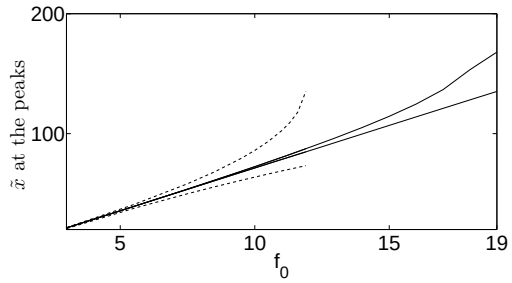

(a) Cubic nonlinear host with $k_3 = 1 \times 10^{-5}$

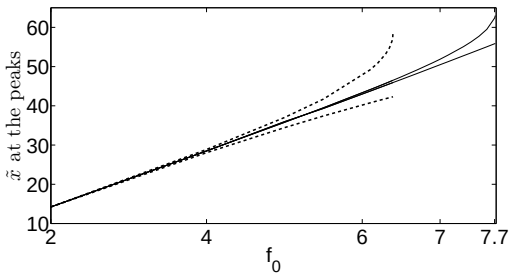

(b) Quintic nonlinear host with $k_5 = 1 \times 10^{-8}$

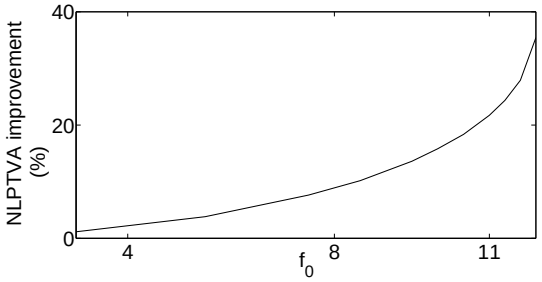

(c) Cubic nonlinear host with $k_3 = 1 \times 10^{-5}$

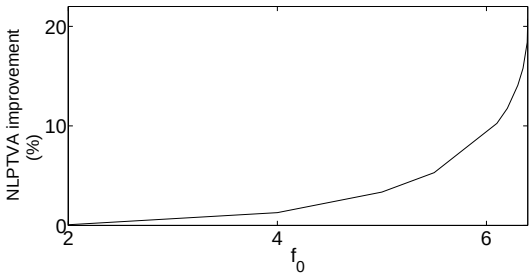

(d) Quintic nonlinear host with $k_5 = 1 \times 10^{-8}$

Figure 6: Peak amplitudes of the NPTVA (solid lines) against LPTVA (dashed lines) for (a) a Duffing nonlinear host with $k_3 = 1 \times 10^{-5}$ (b) a nonlinear host with quintic nonlinear terms with $k_5 = 1 \times 10^{-8}$ at $\alpha = 0.2$; The percentage of improvement brought by the NPTVA with respect to LPTVA for (c) the Duffing (cubic) nonlinear host , (d) the quintic nonlinear host.

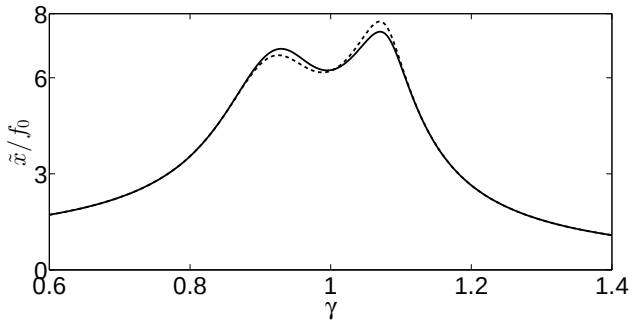

(a) $m_3 = 2.04, m_5 = 0$

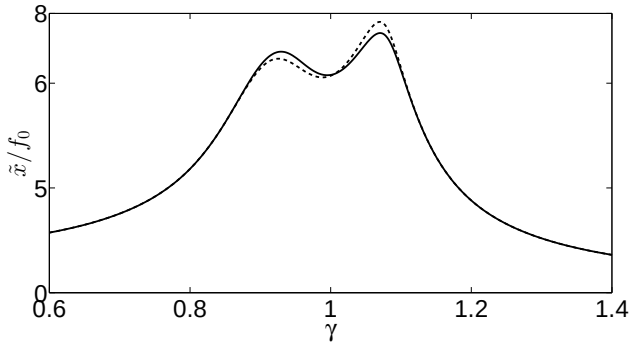

(b) $m_3 = 0, m_5 = 4.12$

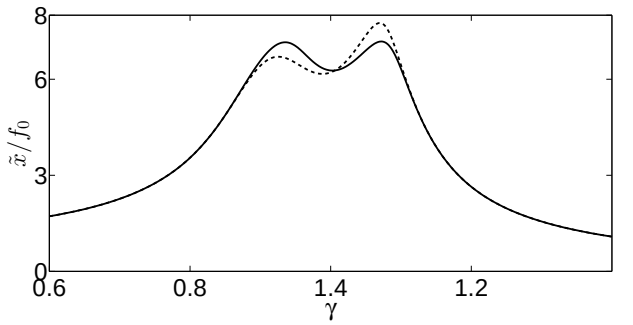

(c) $m_3 = 2.04, m_5 = 4.12$

Figure 7: Frequency response of the host structure with cubic ($k_3 = 1 \times 10^{-5}$) and quintic ($k_5 = 1 \times 10^{-8}$) nonlinearities at $f_0 = 4.1$. (a) NPTVA with cubic nonlinearity; (b) NPTVA with quintic nonlinearity and (c) NPTVA with cubic and quintic nonlinearities. Solid line: NPTVA; dashed line: LPTVA.

cubic and quintic nonlinearities, $\beta_3\widetilde{q}^3 + \beta_5\widetilde{q}^5$, that equal peaks are retrieved. This result suggests that a property of additivity is applicable to the NPTVA. In other words, in case of multiple nonlinearities in the host system, each nonlinearity in the NPTVA can be tuned separately according to the proposed analytical formulas.

Finally, as it was the case for the LPTVA in Figure 2(b), the NPTVA can be suddenly detuned when a detached resonance curve connects with the second resonance peak. However, in case of the cubic NPTVA for instance, this phenomenon is observed only from $f_0 > 20$ and therefore occurs much later than with the LPTVA ($f_0 > 12$).

6 Conclusion

The objective of this paper was to introduce a new nonlinear piezoelectric vibration absorber which targets the mitigation of a specific nonlinear resonance of a mechanical system. The tuning rule used for absorber design relies on a nonlinear principle of similarity, i.e., the nonlinear shunt should be an electrical analog of the host system, and allows us to extend Den Hartog's tuning method to nonlinear systems. Specifically, equal peaks can be maintained in a relatively large range of forcing amplitudes, and this, despite the variation of the resonance frequency of the host system.

A fully analytical design of the nonlinear piezoelectric absorber was proposed for cubic and quintic nonlinearities which combines the results of the homotopy perturbation method with previous exact results obtained for linear systems. Compared to the linear piezoelectric vibration absorber, the nonlinear absorber not only improves mitigation performance but it also extends the range of operation toward larger forcing amplitudes.

Acknowledgments

The authors P. Soltani and G. Kerschen would like to acknowledge the financial support of the Belgian National Science Foundation FRS-FNRS (PDR T.0028.13). G. Kerschen would also like to acknowledge the financial support of the European Union (ERC Starting Grant NoVib 307265).

References

[1] A. J. Fleming and S. O. Reza Moheimani, "Optimal impedance design for piezoelectric vibration control," in *43rd IEEE Conference on Decision and Control*, vol. 3, pp. 2596 – 2601, 2004.

[2] N. W. Hagood and A. von Flotow, "Damping of structural vibrations with piezoelectric materials and passive electrical networks," *Journal of Sound and Vibration*, vol. 146, no. 2, pp. 243–268, 1991.

[3] J. Hogsberg and S. Krenk, "Balanced calibration of resonant shunt circuits for piezoelectric vibration control," *Journal of Intelligent Material, Systems and Structures*, vol. 23, no. 17, pp. 1937–1948, 2012.

[4] K. Yamada, H. Matsuhisa, H. Utsuno, and K. Sawada, "Optimum tuning of series and parallel LR circuits for passive vibration suppression using piezoelectric elements," *Journal of Sound and Vibration*, vol. 329, no. 24, pp. 5036–5057, 2010.

[5] O. Thomas, J. Ducarne, and J. F. Deu, "Performance of piezoelectric shunts for vibration reduction," *Smart Materials and Structures*, vol. 21, p. 015008, 2012.

[6] P. Soltani, G. Kerschen, G. Tondreau, and A. Deraemaeker, "Piezoelectric vibration damping using resonant shunt circuits: an exact solution," *Smart Materials and Structures*, vol. 23, no. 12, p. 125014, 2014.

[7] G. S. Agnes and D. J. Inman, "Nonlinear piezoelectric vibration absorbers," *Smart Materials and Structures*, vol. 5, no. 5, p. 704, 1996.

[8] W. Clark, "Vibration control with state-switching piezoelectric material," *Journal of Intelligent Material Systems and Structures*, vol. 11, pp. 263–271, 2000.

[9] C. Richard, D. Guyomar, Audigier, and G. Ching, "Semi-passive damping using continuous switching of a piezoelectric device," in *Proceedings of SPIE Smart Structures and Materials Conference: Passive Damping and Isolation*, vol. 5386, pp. 414–425, 1999.

[10] J. Ducarne, O. Thomas, and J. F. Deu, "Structural vibration reduction by switch shunting of piezoelectric elements: modeling and optimization," *Journal of Intelligent Material Systems and Structures*, vol. 21, pp. 797–816, 2010.

[11] X. Han, M. Neubauer, and J. Wallaschek, "Improved piezoelectric switch shunt damping technique using negative capacitance," *Journal of Sound and Vibration*, vol. 332, pp. 7–16, 2013.

[12] M. Lallart, L. Yan, Y. C. Wu, and D. Guyomar, "Electromechanical semi-passive nonlinear tuned mass damper for efficient vibration damping," *Journal of Sound and Vibration*, vol. 332, pp. 5696–5709, 2013.

[13] R. Viguie, G. Kerschen, and M. Ruzzene, "Exploration of nonlinear shunting strategies as effective vibration absorbers," in *Proceedings of SPIE Active and Passive Smart Structures and Integrated Systems*, vol. 7288, 2009.

[14] B. Zhou, F. Thouverez, and D. Lenoir, "Essentially nonlinear piezoelectric shunt circuits applied to mistuned bladed disks," *Journal of Sound and Vibration*, vol. 333, pp. 2520–2542, 2014.

[15] A. Vakakis, O. Gendelman, L. A. Bergman, D. M. McFarland, G. Kerschen, and Y. S. Lee, *Nonlinear Targeted Energy Transfer in Mechanical and Structural Systems*, vol. 156 of *Solid Mechanics and Its Applications*. Springer, 2009.

[16] S. Alessandroni, F. Dell'Isola, and M. Porfiri, "A revival of electric analogs for vibrating mechanical systems aimed to their efficient control by pzt actuators," *International Journal of Solids and Structures*, vol. 39, pp. 5295–5324, 2002.

[17] F. D'Annibale, G. Rosi, and A. Luongo, "On the failure of the 'similar piezoelectric control' in preventing loss of stability by nonconservative positional forces," *Zeitschrift fur Angewandte Mathematik und Physik*, vol. in press, 2015.

[18] U. Andreaus, F. Dell'Isola, and M. Porfiri, "Piezoelectric passive distributed controllers for beam flexural vibrations," *Journal of Vibration and Control*, vol. 10, pp. 625–659, 2004.

[19] S. Alessandroni, U. Andreaus, F. Dell'Isola, and M. Porfiri, "A passive electric controller for multimodal vibrations of thin plates," *Computer and Structures*, vol. 83, pp. 1236–1250, 2005.

[20] T. Meeker, "Publication and proposed revision of ANSI/IEEE standard 176-1987, ANSI/IEEE standard on piezoelectricity," *IEEE Transactions on Ultrasonics Ferroelectrics and Frequency Control*, vol. 43, no. 5, pp. 717–772, 1996.

[21] G. Tondreau, A. Deraemaeker, P. Soltani, and G. Kerschen, "Electrical tuned vibration absorber: application of the equal-peak method to linear and non-linear rl piezoelectric shunts," in *25nd International Conference on Adaptive Structures and Technologies*, 2014.

[22] M. Peeters, V. Viguie, G. Serandour, G. Kerschen, and J. C. Golinval, "Nonlinear normal modes, part ii: toward a practical computation using numerical continuation," *Mechanical Systems and Signal Processing*, vol. 23, pp. 195–216, 2009.

[23] G. Habib, T. Detroux, R. Viguié, and G. Kerschen, "Nonlinear generalization of den hartog's equal-peak method," *Mechanical Systems and Signal Processing*, vol. 52, pp. 17–28, 2015.

[24] J. H. He, "Homotopy perturbation technique," *Computer methods in applied mechanics and engineering*, vol. 178, no. 3, pp. 257–262, 1999.

[25] J. H. He, "The homotopy perturbation method for nonlinear oscillators with discontinuities," *Applied Mathematics and Computation*, vol. 151, no. 1, pp. 287–292, 2004.

[26] A. H. Nayfeh, *Perturbation methods*. John Wiley & Sons, 2008.

[27] S. Liao, "Comparison between the homotopy analysis method and homotopy perturbation method," *Applied Mathematics and Computation*, vol. 169, no. 2, pp. 1186–1194, 2005.

Appendix A: Analytical formulas for LPTVAs

The auxiliary parameters in Equations (7) and (9) are:

$$\begin{aligned}
\chi &= \frac{1}{8}\sqrt{64 - 2\,\alpha^2\sqrt{54\,\alpha^4 - 144\,\alpha^2 + 64} + 55\,\alpha^4 - 144\,\alpha^2},\\
\tilde{a} &= \frac{\left(h_0^2 - 1\right)^2}{h_0^6},\\
\tilde{b} &= -2\,\frac{\left(2\,\chi + \alpha^2\right)\left(h_0^2 - 1\right)}{h_0^4},\\
S &= \frac{1}{2}\sqrt{\frac{1}{3\tilde{a}}\left(Q + \frac{\Delta_0}{Q}\right) - \frac{2}{3}p}.
\end{aligned} \tag{A-1}$$

The parameters appearing in the expression of variable S are

$$\begin{aligned}
Q &= \sqrt[3]{\frac{\Delta_1 + \sqrt{\Delta_1^2 - 4\Delta_0^3}}{2}},\\
\Delta_0 &= \tilde{c}^2 - 3\tilde{b}\tilde{d} + 12\tilde{a}\tilde{e},\\
p &= \frac{8\tilde{a}\tilde{c} - 3\tilde{b}^2}{8\tilde{a}^2},
\end{aligned} \tag{A-2}$$

with

$$\begin{aligned}
\Delta_1 &= 2\tilde{c}^3 - 9\tilde{b}\tilde{c}\tilde{d} + 27\tilde{b}^2\tilde{e} + 27\tilde{a}\tilde{d}^2 - 72\tilde{a}\tilde{c}\tilde{e},\\
\tilde{c} &= 5\,\frac{\alpha^4}{{h_0}^2} + \left(\frac{4\chi}{{h_0}^2} - \frac{8}{{h_0}^2}\right)\alpha^2 + \frac{6}{{h_0}^2} - \frac{6}{{h_0}^4},\\
\tilde{d} &= 2\,\chi^3 + \left(4\,\alpha^2 - 2 - \frac{2}{{h_0}^2}\right)\chi - 2\,\frac{\alpha^2}{{h_0}^2} + 2\,\alpha^6 - 2\,\alpha^4,\\
\tilde{e} &= \frac{1}{{h_0}^2}.
\end{aligned} \tag{A-3}$$

To obtain the analytical expressions of the resonant frequencies, we write that the square of the receptance function

$$g_e^2(\gamma_0) = \frac{1 + {\gamma_0}^4 + \left(\delta^2 r^2 - 2\right){\gamma_0}^2}{\left[\begin{array}{c}\delta^4{\gamma_0}^8 + \left(\delta^6 r^2 - 2\,\delta^4 - 2\,\delta^2\right){\gamma_0}^6 +\\ \left(-2\,\delta^4 r^2 - 2\,\alpha^2\delta^2 + \delta^4 + 4\,\delta^2 + 1\right){\gamma_0}^4 +\\ \left(2\,\alpha^2\delta^2 + \delta^2 r^2 + 2\,\alpha^2 - 2\,\delta^2 - 2\right){\gamma_0}^2 + \alpha^4 - 2\,\alpha^2 + 1\end{array}\right]}, \tag{A-4}$$

takes the value h_0^2 at the resonant frequency $\gamma_1 = \gamma_0^2 = (\delta\gamma)^2$ where the expression of h_0 is given in Equation (9). This yields:

$$b_4\gamma_1^4 + b_3\gamma_1^3 + b_2\gamma_1^2 + b_1\gamma_1 + b_0 = 0, \tag{A-5}$$

Equation (A-5), which has too real double roots, can be solved analytically to provide the two resonant frequencies γ_M and γ_N:

$$\gamma_M = \delta\sqrt{-\frac{b_3}{4\,b_4} - \bar{S}}\,,\gamma_N = \delta\sqrt{-\frac{b_3}{4\,b_4} + \bar{S}}. \tag{A-6}$$

where

$$
\begin{aligned}
b_4 &= \delta^4 \\
b_3 &= \delta^6 r^2 - 2\,\delta^4 - 2\,\delta^2, \\
b_2 &= -2\,\delta^4 r^2 - 2\,\alpha^2\delta^2 + \delta^4 + 4\,\delta^2 + 1 - \frac{1}{h_0^2}, \\
b_1 &= 2\,\alpha^2\delta^2 + \delta^2 r^2 + 2\,\alpha^2 - 2\,\delta^2 - 2 - \frac{\delta^2 r^2 - 2}{{h_0}^2}, \\
b_0 &= 1 + \alpha^4 - 2\,\alpha^2 - \frac{1}{h_0^2}, \\
\bar{S} &= \frac{1}{2}\sqrt{\frac{-2}{3}\,\bar{p} + \frac{1}{3b_4}(\bar{Q} + \frac{\bar{\Delta}_0}{\bar{Q}})}, \\
\bar{Q} &= \sqrt[3]{\frac{\bar{\Delta}_1 + (\bar{\Delta}_1^2 - 4\,\bar{\Delta}_0^3)^{\frac{1}{2}}}{2}}, \\
\bar{p} &= \frac{8\,b_2\,b_4 - 3\,{b_3}^2}{8\,{b_4}^2}, \\
\bar{q} &= \frac{8\,b_1\,{b_4}^2 - 4\,b_2\,b_3\,b_4 + {b_3}^3}{8\,{b_4}^3}, \\
\bar{\Delta}_0 &= 12\,b_0\,b_4 - 3\,b_1\,b_3 + {b_2}^2, \\
\bar{\Delta}_1 &= -72\,b_0\,b_2\,b_4 + 27\,b_0\,{b_3}^2 + 27\,{b_1}^2 b_4 - 9\,b_1\,{}_2\,b_3 + 2\,{b_2}^3.
\end{aligned}
\tag{A-7}
$$

Appendix B: Compact formulas for $m_{3\,opt}$ and $m_{5\,opt}$

Equations (33) and (38) can be written in a more compact form:

$$m_{3\,opt} = \frac{\beta_{3\,opt}}{k_3} = \frac{\bar{a}_3 k_3 f_0^2 + \bar{c}_3 + \sqrt{\bar{\mathrm{A}}_3 k_3^2 f_0^4 + \bar{\mathrm{B}}_3 k_3 f_0^2 + \bar{\mathrm{C}}_3}}{k_3 f_0^2}, \tag{B-1}$$

$$m_{5\,opt} = \frac{\beta_{5\,opt}}{k_5} = \frac{\bar{a}_5 k_5 f_0^4 + \bar{c}_5 + \sqrt{\bar{\mathrm{A}}_5 k_5^2 f_0^8 + \bar{\mathrm{B}}_5 k_5 f_0^4 + \bar{\mathrm{C}}_5}}{k_5 f_0^4}, \tag{B-2}$$

where the values of the different parameters are given in the tables below.

Table B-1: Numerical values of the parameters in Equation (B-1) for different α.

α	$\bar{a}_3$	$\bar{c}_3$	$\bar{\mathrm{A}}_3$	$\bar{\mathrm{B}}_3$	$\bar{\mathrm{C}}_3$
0.1	-1.503184524	-0.1770699455e-1	2.268154984	0.1247271699	0.3135376563e-3
0.2	-1.591962280	-0.7034444187e-1	2.533519216	0.513496246	0.4948340502e-2
0.3	-1.656282566	-0.1534938581	2.743390340	1.16798782	0.02356036447
0.4	-1.823596638	-0.2627508006	3.325497592	2.17113406	0.06903798319
0.5	-2.183077347	-0.3883677872	4.757731002	3.708344449	0.1508295382
0.6	-2.681417170	-0.4800720908	7.189999207	5.781337341	0.2304692122

Table B-2: Numerical values of the parameters in Equation (B-2) for different α.

α	$\bar{a}_5$	$\bar{c}_5$	$\bar{\mathrm{A}}_5$	$\bar{\mathrm{B}}_5$	$\bar{\mathrm{C}}_5$
0.1	-1.447232154	-0.1442749395e-3	2.101876664	0.158366940e-2	2.081525819e-8
0.2	-1.444758618	-0.2235879146e-2	2.084664049	0.02496243594	0.4999155549e-5
0.3	-1.557703830	-0.1097104589e-1	2.426771136	0.1291700367	0.1203638480e-3
0.4	-1.806756434	-0.3326314489e-1	3.264356368	0.4320700751	0.1106436807e-2
0.5	-2.247729834	-0.7582597454e-1	5.05230223	1.155667704	0.5749578415e-2
0.6	-3.210472285	-.1372445401	10.30715585	2.814812586	0.1883606378e-1